LENS GALAXY PROPERTIES OF SBS 1520+530: INSIGHTS FROM KECK SPECTROSCOPY AND AO IMAGING

M. W. AUGER, C. D. FASSNACHT, AND K. C. WONG

Department of Physics, University of California, 1 Shields Avenue, Davis, CA 95616; mauger@physics.ucdavis.edu, fassnacht@physics.ucdavis.edu

D. THOMPSON

Large Binocular Telescope Observatory, University of Arizona, 933 North Cherry Avenue, Tucson, AZ 85721

AND

K. MATTHEWS AND B. T. SOIFER

Caltech Optical Observatories, California Institute of Technology, Pasadena, CA 91125

Received 2007 June 27; accepted 2007 October 9

ABSTRACT

We report on an investigation of the SBS 1520+530 gravitational lens system. We have used archival *Hubble Space Telescope* (*HST*) imaging, Keck spectroscopic data, and Keck adaptive optics (AO) imaging to study the lensing galaxy and its environment. The AO imaging has allowed us to fix the lens galaxy properties with a high degree of accuracy when performing the lens modeling, and the data indicate that the lens has an elliptical morphology and perhaps a disk. The new spectroscopic data suggest that previous determinations of the lens redshift may be incorrect, and we report an updated, although inconclusive, value $z_{\rm lens} = 0.761$. We have also spectroscopically confirmed the existence of several galaxy groups at approximately the redshift of the lens system. We create new models of the lens system that explicitly account for the environment of the lens, and we also include improved constraints on the lensing galaxy from our AO imaging. Lens models created with these new data can be well fit with a steeper than isothermal mass slope ($\alpha = 2.29$, where $\rho \propto r^{-\alpha}$) if H_0 is fixed at 72 km s^{-1} Mpc^{-1}; isothermal models require $H_0 \sim 50$ km s^{-1} Mpc^{-1}. The steepened profile may indicate that the lens is in a transient perturbed state caused by interactions with a nearby galaxy.

Subject heading: galaxies: individual (SBS 1520+530)

1. INTRODUCTION

The strong gravitational lens system SBS 1520+530 (hereafter SBS 1520) was first investigated by Chavushyan et al. (1997), who found that the system consists of a pair of images of a broad absorption-line quasar ($z_{\rm src} = 1.855$) separated by 1.6″. The lensing galaxy was soon detected with adaptive optics (AO) imaging (Crampton et al. 1998) and was assumed to be at the redshift of one of two absorption-line systems seen in the spectra of the quasar images. Burud et al. (2002) attempted to deconvolve the lens spectrum from the quasar spectra and found the redshift of the lens to be $z_{\rm lens} = 0.717$. This redshift is broadly consistent with a photometric redshift determined by Faure et al. (2002). Furthermore, the lens was found to lie along the line of sight to a photometrically identified cluster of galaxies that is expected to be at approximately the same redshift as the lens (Burud et al. 2002; Faure et al. 2002).

Optical monitoring campaigns have led to the measurement of a time delay between the quasar images of ∼130 days (Burud et al. 2002; Khamitov et al. 2006). This time delay provides an additional constraint for determining the mass slope of the lens galaxy (e.g., Rusin et al. 2003) and allows a value of the Hubble constant to be determined for the system ($H_0 = 51$ km s^{-1} Mpc^{-1} assuming an isothermal mass profile; Burud et al. 2002). Note, however, that the mass slope and, thus, the value of H_0 depend on the environment surrounding the lens system (e.g., Dobke et al. 2007; Auger et al. 2007). An incorrect understanding of the mass distribution and environment of the lens might account for the anomalously low value of H_0 obtained for SBS 1520 compared to other lens systems (e.g., Koopmans et al. 2003; York et al. 2005) and the *Wilkinson Microwave Anisotropy Probe* (Spergel et al. 2007) and *Hubble Space Telescope* (*HST*) Key Project (Freedman et al. 2001) results.

In this paper we present new Keck AO and archival *HST* imaging of the lens system that indicates the lensing galaxy may have a disk component. We also present a spectroscopic investigation of the lens environment and provide a new analysis of the lensing galaxy's spectrum, which results in an updated lens redshift of $z_{\rm lens} = 0.761$. We discuss the implications of these new observational data on previous analyses performed with SBS 1520 and suggest that, in spite of some complexity, this lens provides an interesting platform to investigate dark matter interactions in dense environments.

2. IMAGING

High-resolution imaging of SBS 1520 at 2.12 μm (K_p band) was obtained on 2006 May 2 with the Near Infrared Camera 2 (NIRC2; K. Matthews et al. 2008, in preparation) behind the AO bench on the W. M. Keck II telescope. The NIRC2 narrow camera was used for the imaging, which provides a field of view of $10'' \times 10''$ and a pixel scale of 9.94 mas pixel^{-1}. The data were taken in nine 90 s exposures with a small dither between each exposure to facilitate good sky background subtraction during the reduction process. A sodium laser guide star was used to correct for the atmospheric turbulence, and a $r = 12$ star, 15″ from SBS 1520, was used for tip-tilt correction.

The data were reduced within IRAF[1] using a double-pass reduction algorithm. The first pass is used to determine the positions

---

[1] IRAF (Image Reduction and Analysis Facility) is distributed by the National Optical Astronomy Observatory, which is operated by AURA, Inc., under cooperative agreement with the National Science Foundation.
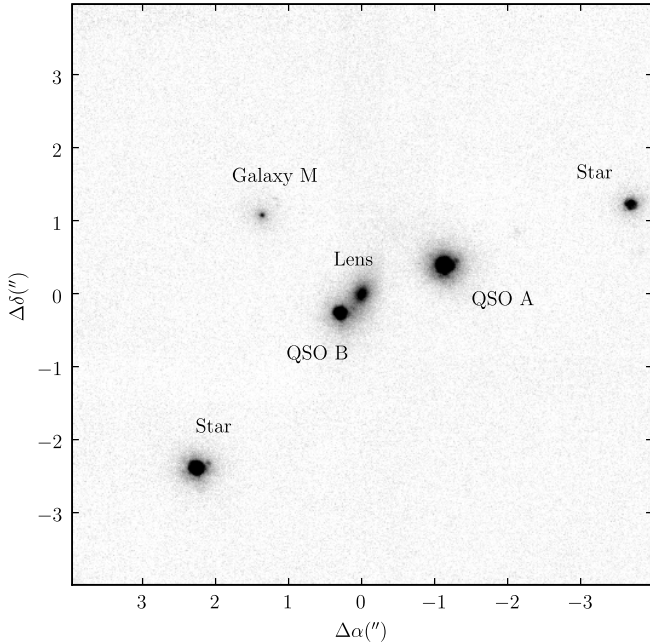
Fig. 1.—Keck NIRC2 AO *K*-band image of the SBS 1520 lens system. The image is centered on the lensing galaxy, and two field stars are indicated. The galaxy to the northeast of the lens is denoted galaxy M. The lensed quasar components are also indicated. The resolution of the image is 0.05″.

of the objects on the sky, which are then masked out during the second pass where the usual sky subtraction with temporally adjacent frames is carried out. Bad pixel and cosmic-ray masks are generated during this process, and these masks are then used to construct weight maps. The individual exposures are combined using the weight maps and the `drizzle` package (Fruchter & Hook 2002), which also corrects the data for the geometric distortions across the NIRC2 camera to provide precise relative astrometry. The point-source full width at half-maximum (FWHM) in the final drizzled image is 54 mas.

The inner 8″ of the AO imaging is shown in Figure 1, clearly showing the two lensed quasar images, the lensing galaxy, and a nearby galaxy. The high resolution and sensitivity of the observations allow us to determine the morphological parameters of the lensing galaxy with a high degree of confidence. The A and B images of the quasar were fitted and subtracted using an empirical point-spread function (PSF) determined from the star to the southeast of the lens (Fig. 2*a*); the *K*-band image of the lens shows an early-type morphology, perhaps with a disk. A best-fit galaxy model was then determined for the lensing galaxy using a nonlinear fitting code to model the lens with a Sérsic model convolved with the empirical PSF. The residuals from this model are shown in Figure 2*b*; the best-fit Sérsic index is $n = 2.7$, and the effective radius is determined to be $r_e = 0.49''$. The ellipticity from the model is found to be 0.44 at a position angle of 156°.

We have also obtained *HST* WFPC2 and NICMOS archival data for SBS 1520 (*HST* GO Programs 8175, 7495, and 7887; PI: E. Falco). The imaging data consist of 2100 s with the F555W filter and 1600 s with F814W using WFPC2, and 2816 s with F160W and the NIC2 camera. These data were reduced using the `multidrizzle`[2] package (Koekemoer et al. 2002), and galaxy properties were measured using SExtractor (Bertin & Arnouts 1996). The relative positions of the sources used in our analysis

---

[2] `Multidrizzle` is a product of the Space Telescope Science Institute, which is operated by AURA for NASA.
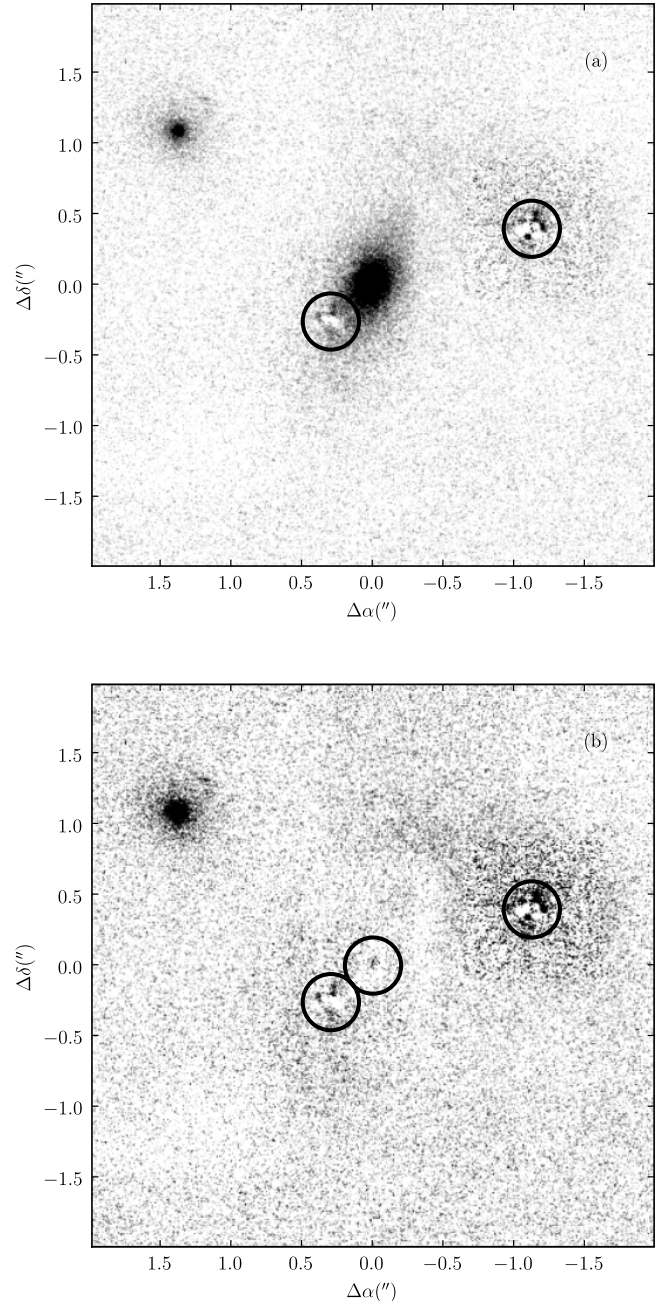

Fig. 2.—Keck AO *K*-band image of SBS 1520 with (*a*) the quasar images subtracted and (*b*) the quasar images and the Sérsic model of the lensing galaxy subtracted. Circles indicate the centers of the subtracted components; note that a faint core is noticeable in the residuals of the galaxy.

have been measured from the NIRC2 imaging if the objects are in the NIRC2 field of view; otherwise, the F814W imaging has been used. The lens system was placed at the center of the PC chip for the WFPC2 data and in the center of the NICMOS field, providing complete coverage out to 16″ for the WFPC2 fields (see Fig. 3) and 12″ for the NICMOS field. The object ∼1.8″ to the northeast of the lens is not resolved in conventional ground-based imaging but is revealed to be a galaxy in AO and *HST* imaging, with a FWHM approximately 30% larger than the PSF. Following Burud et al. (2002) we will denote this galaxy as galaxy M.

3. SPECTROSCOPY

We have obtained spectroscopic observations of SBS 1520 using the Echellette Spectrograph and Imager (ESI; Sheinis et al.
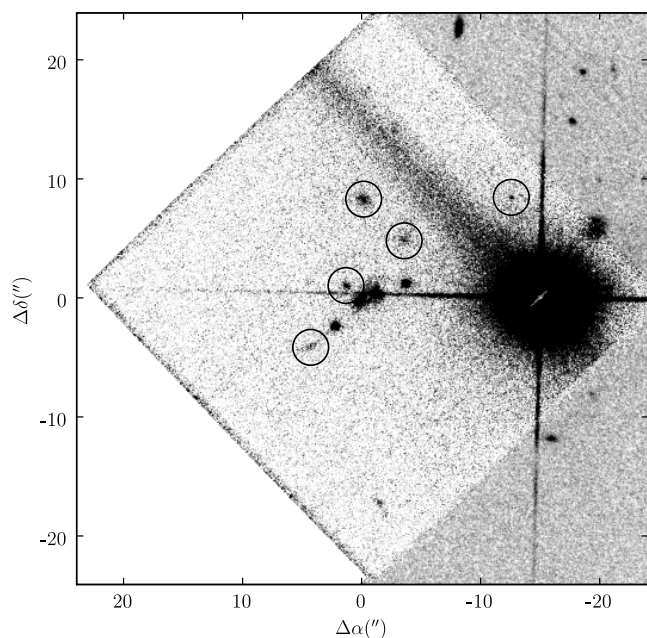
Fig. 3.—WFPC2 F814W image of the SBS 1520 field. All galaxies within 16″ of the lens are indicated with circles and have been explicitly included in the lens modeling. The bright star 15″ west of the lens was used for the AO imaging.
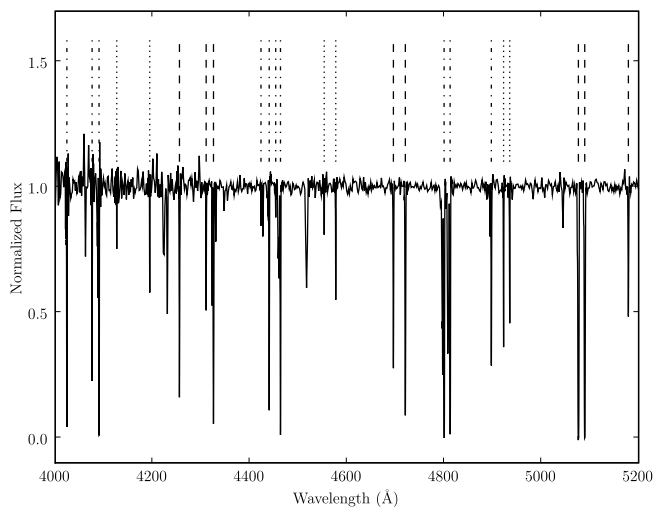

Fig. 4.—Portion of the spectrum extracted from the A component; there are four absorption systems seen in the SBS 1520 quasar spectra. Prominent features from the $z = 0.717$ (*dash-dotted lines*), $z = 0.760$ (*dotted lines*), and $z = 0.815$ (*dashed lines*) systems are indicated; most of these features are Fe and Mg lines. The spectrum has been divided by the continuum, and several of the Mg II lines are seen to be saturated.

2002) on the Keck II telescope and the Low-Resolution Imaging Spectrograph (LRIS; Oke et al. 1995) on the Keck I telescope. Our primary lens spectroscopy was obtained with ESI on 2000 July 3 in conditions with thin cirrus and approximately 0.8″ seeing. Four 1800 s exposures were observed with a 0.75″ slit. The ESI slit was oriented to run through both quasar images and through the lensing galaxy. Two LRIS slit-mask observations were made on 2004 June 15 in nonphotometric conditions with approximately 1.5″ seeing. The purpose of the LRIS observations was to mea- sure redshifts for both the lensing galaxy and nearby galaxies. The 831/9200 grating, with dispersion 0.9 Å pixel^{-1}, was used on the red arm of the spectrograph, and the blue arm employed the 600/4000 grism with dispersion 0.63 Å pixel^{-1}. Four exposures of 1800 s were obtained for each mask, although one exposure of the second mask was discarded due to poor transparency. Both of the slit masks contained a slit placed over the lens system in the same orientation as the ESI slit, providing seven good LRIS ex- posures of 1800 s for the lens system.

3.1. *Data Reduction*

The LRIS data were reduced using a custom automated pipe- line written in Python (M. W. Auger 2008, in preparation). The pipeline removes the instrumental bias and overscan regions of the LRIS CCDs, corrects for amplifier gain offsets, and flat fields the data from the red arm of the spectrograph. The program then automatically determines a wavelength solution from arc lamp exposures and skylines, corrects for telluric absorption features with an air-mass-scaled model of the typical absorption at Keck, performs an "optimal" background subtraction (Kelson 2003), and resamples and co-adds the two-dimensional spectra to a con- stant wavelength-scale grid. The pipeline also searches each slit for spectral traces or emission lines and performs an aperture- weighted extraction. The extracted spectra were cross-correlated with galactic and stellar template spectra to determine redshifts for the science targets. All of these redshifts were then verified by hand; several were discarded due to poor quality spectra, while others were corrected by manually identifying features.

The ESI data were reduced with a modified version of the Python scripts used to reduce the LRIS data. A star was observed at several positions along the slit, and the traces of the star were used to straighten the echelle dispersion orders. A wavelength solution was determined from HgNe, CuAr, and Xe arc lamp observations. The science data and an observation of the spectro- photometric standard star HZ 44 (Oke 1990) were then straight- ened, and the night-sky background was subtracted. The spectrum of HZ 44 was then extracted, and an atmospheric absorption and instrumental response model was created. The SBS 1520 quasar spectra were then traced and extracted. The galaxy spectrum was extracted by defining a Gaussian aperture with a FWHM of 1 pixel centered slightly off of the position of the lens galaxy to mini- mize the shot noise from the quasar light. The extracted spectra from the four exposures were then co-added, and a smoothed ver- sion of the galaxy spectrum was created by convolving the galaxy spectrum with a Gaussian kernel of width $\sigma = 100$ km s^{-1}. We also extracted the galaxy spectrum by modeling the quasar images and lens galaxy in a method similar to Burud et al. (2002; see also Courbin et al. 2000; Eigenbrod et al. 2007). Two stars (shown in Fig. 1) were observed on the ESI and LRIS slits along with the lens system to help define the PSF, but we found that our ob- servations did not have sufficient sensitivity to adequately model the galaxy and quasar spectra without substantial artifacts.

3.2. *SBS 1520 Quasar and Lens Spectra*

Previous observations of SBS 1520 have revealed several line- of-sight absorption systems present in the quasar spectra at $z \approx 0.717$ and $z \approx 0.815$ (Chavushyan et al. 1997; Burud et al. 2002). Burud et al. (2002) found evidence for Ca II K and H ab- sorption features associated with the $z = 0.717$ system in the two quasar spectra and also found these lines in a spectrum of the lens galaxy obtained by deconvolving the lens spectrum from the qua- sar spectra. The absence of Ca II features associated with the $z = 0.815$ system led those authors to assign the lens galaxy the redshift $z = 0.717$. Our data confirm the absorption systems seen at $z = 0.717$ and $z = 0.815$, but the quasar spectra also reveal a Mg and Fe absorption system at $z = 0.760$ and a C IV absorption system at $z = 1.728$ (Fig. 4). Furthermore, we have also found

and use the isothermal models of Burud et al. (2002). The mass slope modeled in our analysis is steeper than expected for early-type galaxies (e.g., Koopmans et al. 2006), but the presence of a nearby galaxy, galaxy M, suggests that SBS 1520 may be undergoing interaction-induced steepening (e.g., Dobke et al. 2007). Read et al. (2007) have used pixelated mass models to model SBS 1520 and find a nearly isothermal profile, $\alpha = 1.95$. These models are able to account for "shape degeneracies" that may also affect interpretations of time delays (Saha & Williams 2006), although the analysis of Saha & Williams (2006) indicates that shape degeneracies are probably not important for SBS 1520. Note that Read et al. (2007) do not explicitly model the lens environment, and they are therefore measuring the joint projected mass slope of the lens and environment. If the lens is not near the (projected) group center, the inferred mass slope would be shallower than the true mass slope.

5. CONCLUSIONS

We have obtained deep AO imaging and optical spectroscopy of the time-delay lens SBS 1520. The AO imaging has allowed us to fix the lens galaxy properties with a high degree of precision when performing the lens modeling, and the data indicate that the lens has an elliptical morphology and perhaps a disk. The new spectroscopic data suggest that previous determinations of the lens redshift may be incorrect, and the data also allow us to quantify the lensing contribution of several groups in the immediate foreground and background of the lens. Lens models created with these new data can be well fit with a steeper than isothermal mass slope ($\alpha = 2.29$) if H_0 is fixed at $72 \, \mathrm{km \, s^{-1} \, Mpc^{-1}}$; isothermal models require $H_0 \sim 50 \, \mathrm{km \, s^{-1} \, Mpc^{-1}}$. Dobke et al. (2007) found that galaxies in overdense environments might have steeper than isothermal mass slopes caused by interactions with other galaxies (see also Auger 2008). This suggests an interpretation that we are observing transient steepening of the mass profile due to galaxy-galaxy interactions, and indicates that other lens systems that have obtained anomalously low values of H_0 may lie in overdense regions and near an interacting galaxy (e.g., B1600+434; Koopmans et al. 2000; Auger et al. 2007). Alternatively, SBS 1520 can be modeled in a manner consistent with an isothermal profile and $H_0 = 64 \, \mathrm{km \, s^{-1} \, Mpc^{-1}}$ if the lens is modeled by a pixelated mass distribution and jointly modeled with other lens systems (Read et al. 2007). These models indicate that twisting ellipticity, triaxial projection effects, or other shape degeneracies may be affecting the parametric analyses of SBS 1520 (Saha & Williams 2006).

However, there are still several ambiguities in the data that need to be resolved before making definitive claims about the profile of SBS 1520, particularly in the context of the interaction-induced steepening scenario. While we have argued that the lens redshift is likely to be $z = 0.761$ and not $z = 0.717$, the data are not conclusive. Furthermore, our modeling has assumed that all of the neighbor galaxies are at the group redshift; if this is the case, the $z = 0.76$ group centroid would be pulled closer to the lens and the group would therefore provide a larger contribution to the lens model. If this is not the case, the neighboring galaxies might have a smaller impact on the lens model. This is particularly important for galaxy M, as this is the neighboring galaxy that most affects the lens model but also has colors least like the lens galaxy compared to the other field galaxies. It is also important to verify that at least one of the neighboring galaxies is at the same redshift as the lens, because this is a requirement of the interaction-driven steepening hypothesis. Finally, obtaining a dynamical estimate of the lens mass would help to further constrain models and potentially distinguish between shape degeneracies and the mass slope degeneracy.

REFERENCES

Adelman-McCarthy, J. K., et al. 2008, ApJS, in press (arXiv: 0707.3413v2)
Auger, M. W. 2008, MNRAS, 383, L40
Auger, M. W., Fassnacht, C. D., Abrahamse, A. L., Lubin, L. M., & Squires, G. K. 2007, AJ, 134, 668
Bertin, E., & Arnouts, S. 1996, A&AS, 117, 393
Burud, I., et al. 2002, A&A, 391, 481
Chavushyan, V. H., Vlasyuk, V. V., Stepanian, J. A., & Erastova, L. K. 1997, A&A, 318, L67
Churchill, C. W., Kacprzak, G. G., & Steidel, C. C. 2005, in IAU Colloq. 199, Probing Galaxies through Quasar Absorption Lines, ed. P. R. Williams, C.-G. Shu, & B. Menard (Cambridge: Cambridge Univ. Press), 24
Courbin, F., Magain, P., Kirkove, M., & Sohy, S. 2000, ApJ, 529, 1136
Crampton, D., Schechter, P. L., & Beuzit, J.-L. 1998, AJ, 115, 1383
Dobke, B. M., King, L. J., & Fellhauer, M. 2007, MNRAS, 377, 1503
Eigenbrod, A., Courbin, F., & Meylan, G. 2007, A&A, 465, 51
Faure, C., Courbin, F., Kneib, J. P., Alloin, D., Bolzonella, M., & Burud, I. 2002, A&A, 386, 69

Freedman, W. L., et al. 2001, ApJ, 553, 47
Fruchter, A. S., & Hook, R. N. 2002, PASP, 114, 144
Keeton, C. R. 2001, preprint (astro-ph/0102340)
Kelson, D. D. 2003, PASP, 115, 688
Khamitov, I. M., Bikmaev, I. F., Aslan, Z., Sakhibullin, N. A., Vlasyuk, V. V., Zheleznyak, A. P., & Zakharov, A. F. 2006, Astron. Lett., 32, 514
Koekemoer, A. M., Fruchter, A. S., Hook, R. N., & Hack, W. 2002, in 2002 *HST* Calibration Workshop, Hubble after the Installation of the ACS and the NICMOS Cooling System, ed. S. Arribas, A. Koekemoer, & B. Whitmore (Baltimore: STScI), 337
Koopmans, L. V. E., de Bruyn, A. G., Xanthopoulos, E., & Fassnacht, C. D. 2000, A&A, 356, 391
Koopmans, L. V. E., Treu, T., Bolton, A. S., Burles, S., & Moustakas, L. A. 2006, ApJ, 649, 599
Koopmans, L. V. E., Treu, T., Fassnacht, C. D., Blandford, R. D., & Surpi, G. 2003, ApJ, 599, 70
Oke, J. B. 1990, AJ, 99, 1621

Oke, J. B., et al. 1995, PASP, 107, 375

Read, J. I., Saha, P., & Macciò, A. V. 2007, ApJ, 667, 645

Rusin, D., Kochanek, C. S., & Keeton, C. R. 2003, ApJ, 595, 29

Saha, P., & Williams, L. L. R. 2006, ApJ, 653, 936

Sheinis, A. I., Bolte, M., Epps, H. W., Kibrick, R. I., Miller, J. S., Radovan, M. V., Bigelow, B. C., & Sutin, B. M. 2002, PASP, 114, 851

Spergel, D. N., et al. 2007, ApJS, 170, 377

Treu, T., & Koopmans, L. V. E. 2002, MNRAS, 337, L6

Williams, L. L. R., & Saha, P. 2000, AJ, 119, 439

Wisotzki, L., Becker, T., Christensen, L., Helms, A., Jahnke, K., Kelz, A., Roth, M. M., & Sanchez, S. F. 2003, A&A, 408, 455

Wucknitz, O. 2002, MNRAS, 332, 951

York, T., Jackson, N., Browne, I. W. A., Wucknitz, O., & Skelton, J. E. 2005, MNRAS, 357, 124